Supplement of Atmos. Chem. Phys., 19, 7939–7954, 2019
https://doi.org/10.5194/acp-19-7939-2019-supplement

Supplement of

Aerosol pH and its driving factors in Beijing

Jing Ding et al.

Correspondence to: Pusheng Zhao (pszhao@ium.cn)

1. Thermodynamic model validation: comparisons of predicted and measured NH_3, HNO_3, HCl, NH_4^+, NO_3^-, Cl^-, $\varepsilon(NH_4^+)$, $\varepsilon(NO_3^-)$, and $\varepsilon(Cl^-)$ in four seasons in Beijing.

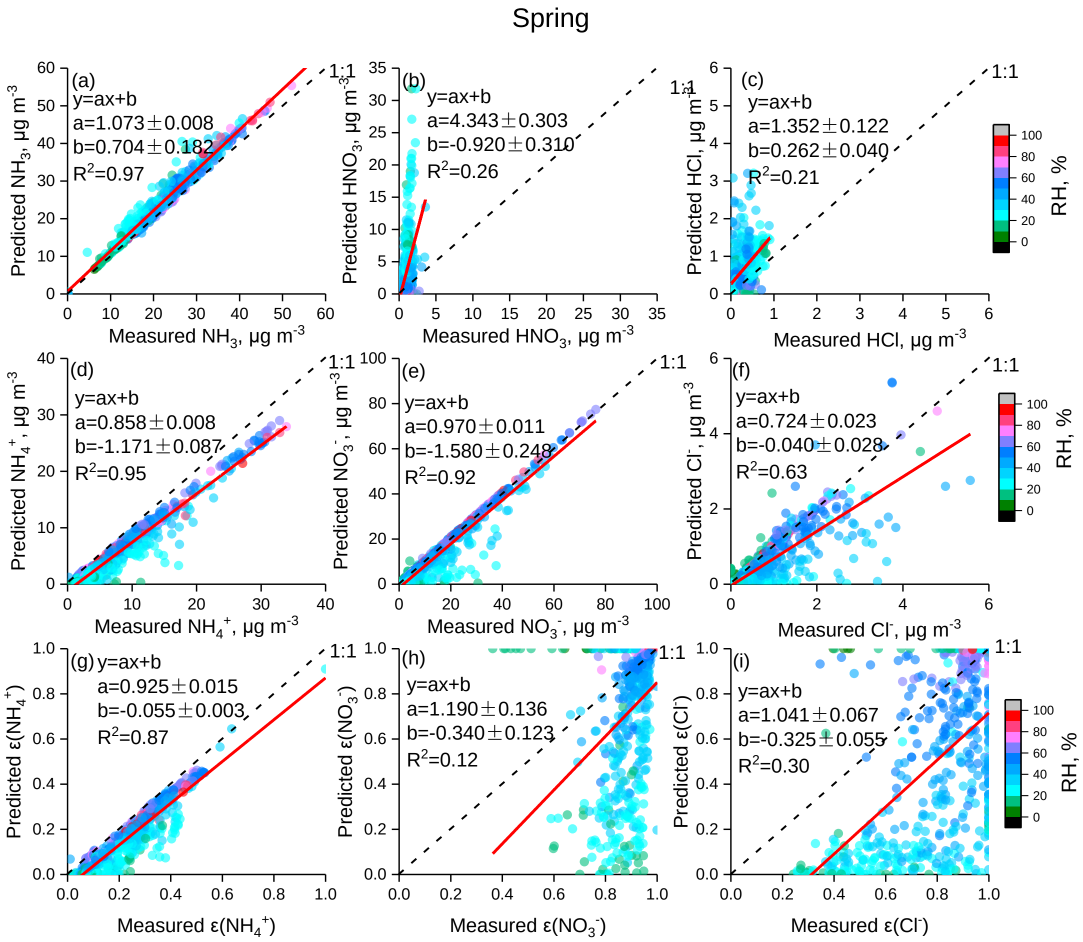

Figure S1. Comparisons of predicted and measured NH_3, HNO_3, HCl, NH_4^+, NO_3^-, Cl^-, $\varepsilon(NH_4^+)$, $\varepsilon(NO_3^-)$, and $\varepsilon(Cl^-)$ coloured by RH in spring.

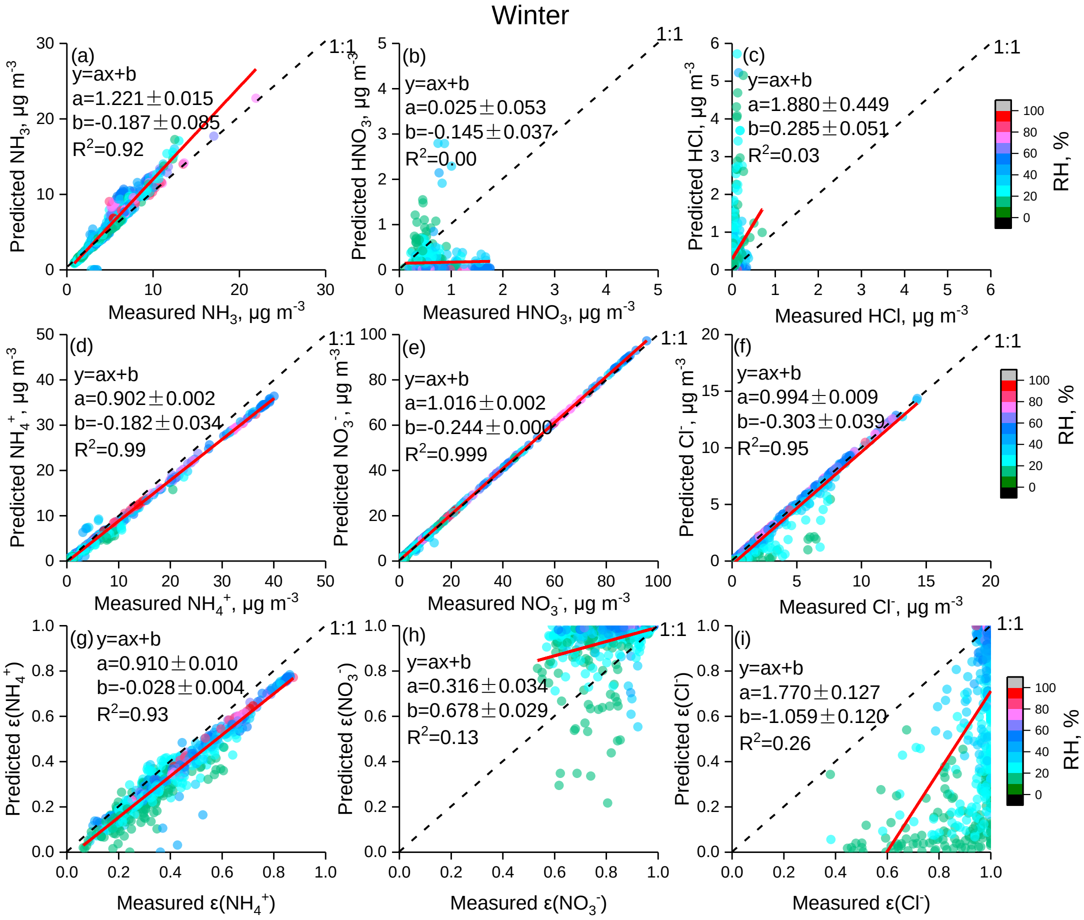

Figure S2. Comparisons of predicted and measured NH_3, HNO_3, HCl, NH_4^+, NO_3^-, Cl^-, $\varepsilon(NH_4^+)$, $\varepsilon(NO_3^-)$, and $\varepsilon(Cl^-)$ coloured by RH in winter.

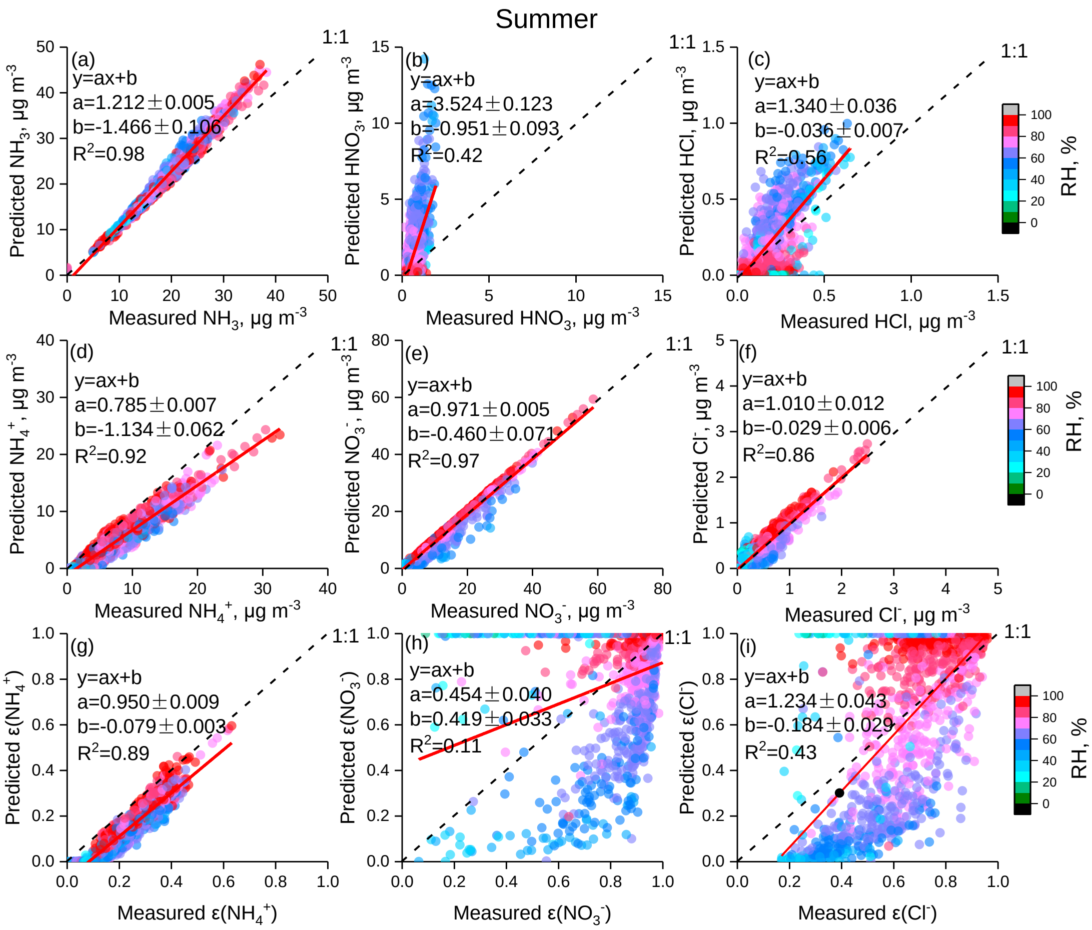

Figure S3. Comparisons of predicted and measured NH_3, HNO_3, HCl, NH_4^+, NO_3^-, Cl^-, $\varepsilon(NH_4^+)$, $\varepsilon(NO_3^-)$, and $\varepsilon(Cl^-)$ coloured by RH in summer.

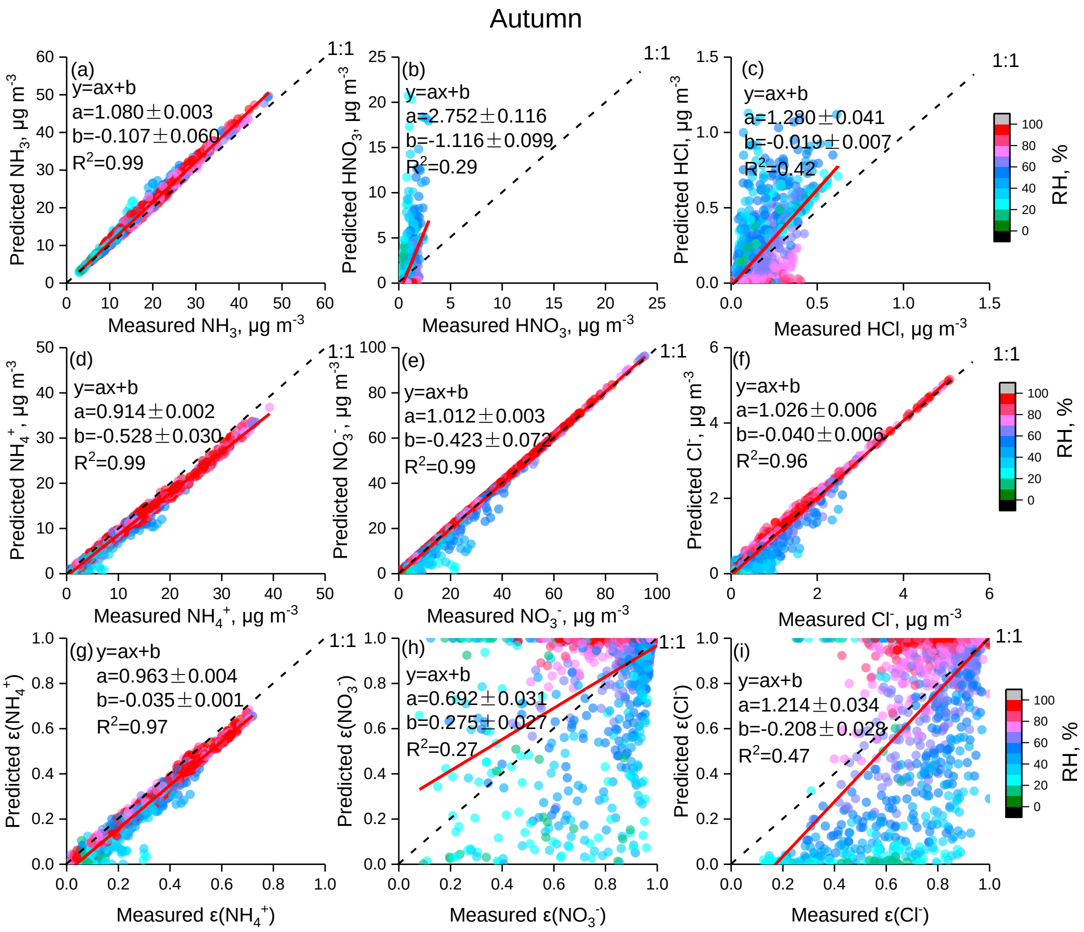

Figure S4. Comparisons of predicted and measured NH_3, HNO_3, HCl, NH_4^+, NO_3^-, Cl^-, $\varepsilon(NH_4^+)$, $\varepsilon(NO_3^-)$, and $\varepsilon(Cl^-)$ coloured by RH in autumn.

2. Relationship between $PM_{2.5}$ pH and mass concentrations of $PM_{2.5}$, SO_4^{2-}, and NO_3^-

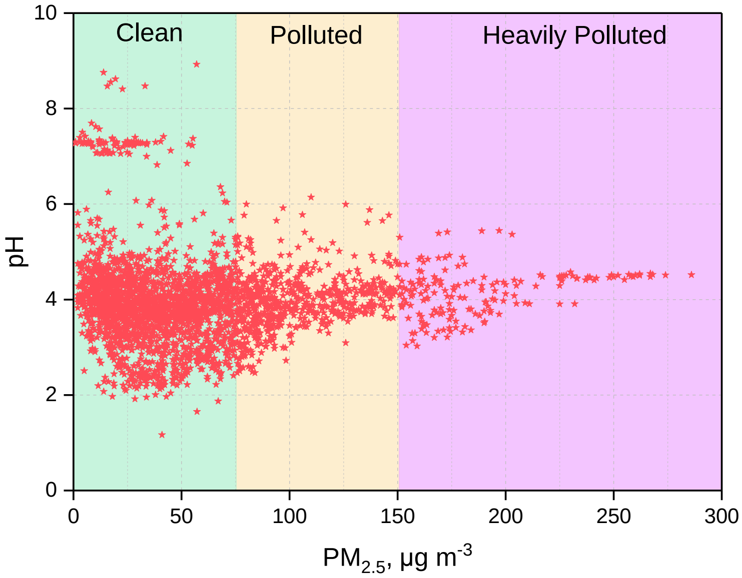

Figure S5. Relationship between $PM_{2.5}$ mass concentration and $PM_{2.5}$ pH (data at RH≤30% were excluded).

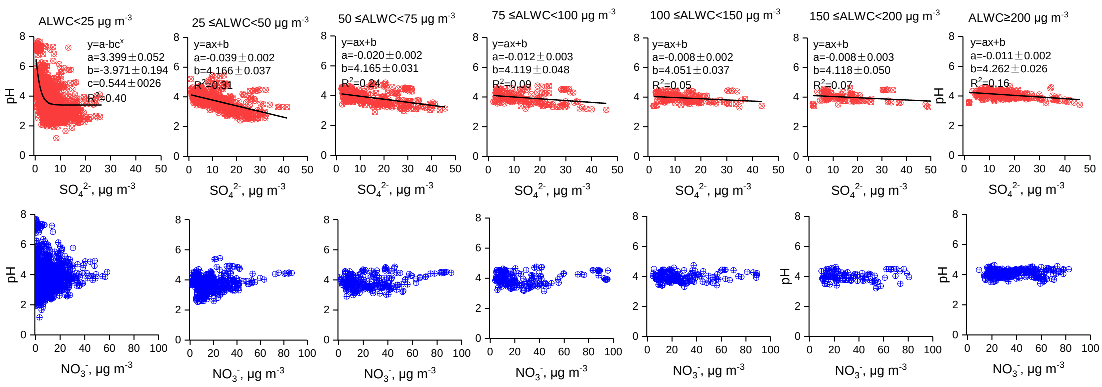

Figure S6. Relationship between mass concentrations of SO_4^{2-} and NO_3^- and $PM_{2.5}$ pH at different ALWC levels.

3. Sensitivity tests of H_{air}^+, aerosol liquid water content, and $PM_{2.5}$ pH to SO_4^{2-}, TNO_3, TNH_3, Ca^{2+}, and meteorological parameters (RH and T) in all four seasons

Table S1. Average value and range of input variables for sensitivity tests over four seasons.

Spring	SO_4^{2-} µg m^{-3}	TNH_3 µg m^{-3}	TNO_3, µg m^{-3}	RH %	T ℃	Ca^{2+} µg m^{-3}	TCl µg m^{-3}	Na^+ µg m^{-3}	K^+ µg m^{-3}	Mg^{2+} µg m^{-3}
Average input	8.4	25.7	13.5	52	20.9	2.2	1.1	0.2	0.34	0.3
Ranges	3.0~41.4	0.1~33.9	0.4~77.6	30~92	10.0~33.3	0.1~11.2				
Winter										
Averaged	7.3	12.2	14.3	52	2.7	0.2	3.0	0.4	1.0	0.2
Ranges	2.0~34.6	1.3~46.7	0.8~49.3	30~94	-8.7~16.2	0.01~0.7				
Summer										
Averaged	8.6	26.8	10.2	74	26.1	0.5	0.6	0.6	0.2	0.1
Ranges	0.6~40.1	1.2~69.6	0.3~59.8	30~97	14.2~38.1	0.02~2.9				
Autumn										
Averaged	9.3	27.8	20.3	72	16.4	0.4	1.0	0.3	0.2	0.1
Ranges	0.3~54.7	3.2~67.5	0.2~90.5	30~97	-1.1~33.3	0.02~2.3				

Table S2. Sensitivity of ALWC and H_{air}^+ to SO_4^{2-}, TNO_3, TNH_3, Ca^{2+}, RH, and T. A larger magnitude of the relative standard deviation (RSD) represents a larger impact derived from variations in variables.

Impact Factor		SO_4^{2-}	TNO_3	TNH_3	Ca^{2+}	RH	T
Spring	RSD-ALWC	50.5%	53.4%	2.9%	31.7%	122%	13.1%
	RSD-H_{air}^+	223%	34.4%	26.8%	72.3%	115%	49.5%
Winter	RSD-ALWC	33.8%	28.7%	14.2%	1.9%	103%	3.5%
	RSD-H_{air}^+	431%	431%	187.4%	11.3%	136%	74.1%
Summer	RSD-ALWC	49.4%	46.0%	6.9%	9.0%	104%	10.8%
	RSD-H_{air}^+	131%	29.9%	78.1%	18.1%	44.6%	33.9%
Autumn	RSD-ALWC	32.8%	58.1%	9.9%	3.3%	77.6%	5.5%
	RSD-H_{air}^+	171%	126.7%	333.1%	9.3%	106%	59.6%

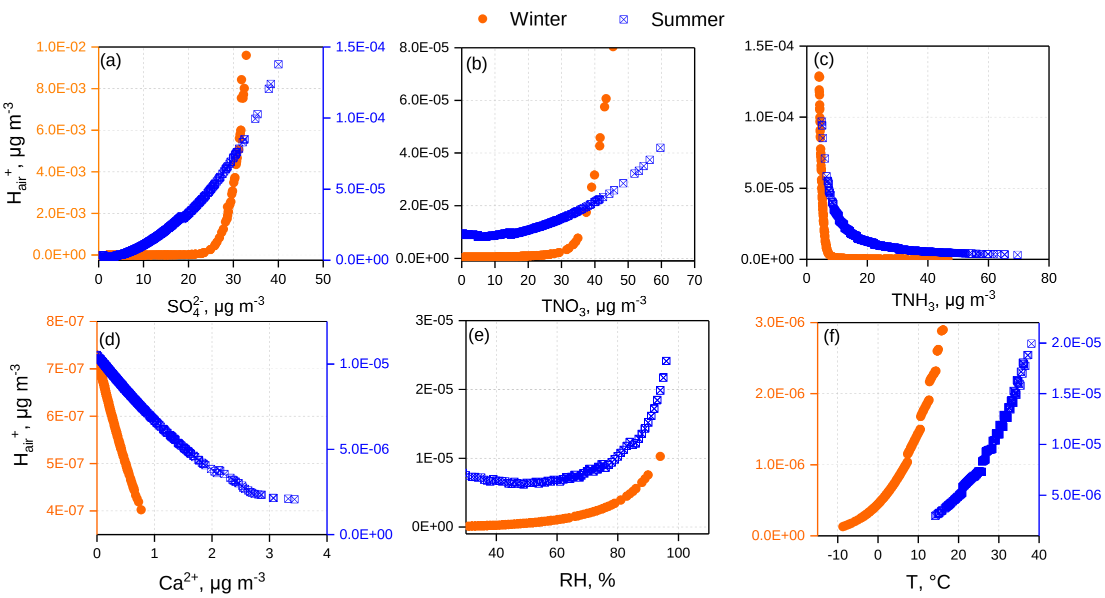

Figure S7. Sensitivity tests of H_{air}^{+} to SO_4^{2-}, TNO_3, TNH_3, Ca^{2+}, and meteorological parameters (RH and T) in summer and winter.

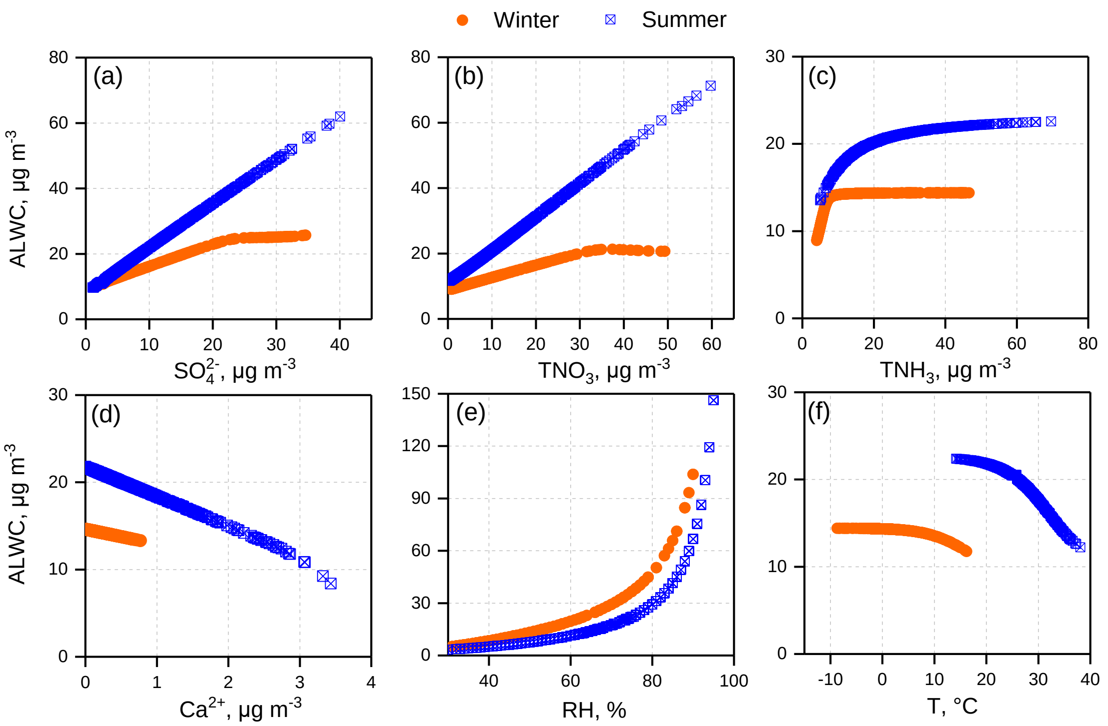

Figure S8. Sensitivity tests of ALWC to SO_4^{2-}, TNO_3, TNH_3, Ca^{2+}, and meteorological parameters (RH and T) in summer and winter.

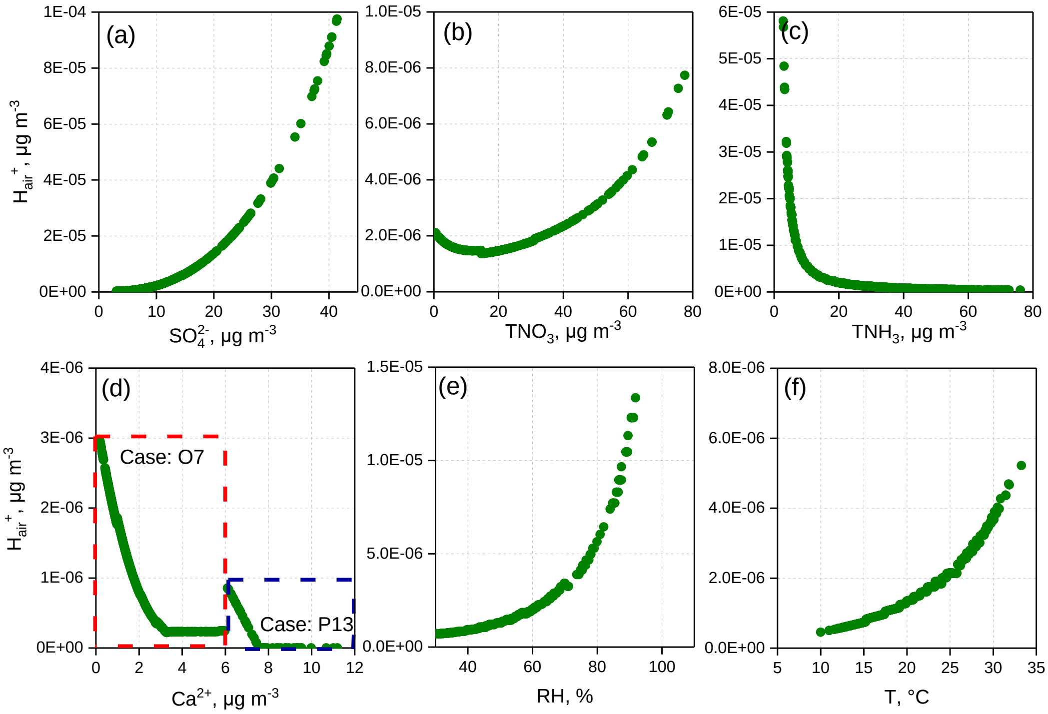

Figure S9. Sensitivity tests of H_{air}^+ to SO_4^{2-}, TNO_3, TNH_3, Ca^{2+}, and meteorological parameters (RH and T) in spring. For the sensitivity of H_{air}^+ to Ca^{2+}, in ISORROPIA-II, subroutine O7 was automatically called when the Ca^{2+} mass concentration was low and the subroutine P13 was automatically called when the Ca^{2+} mass concentration was high.

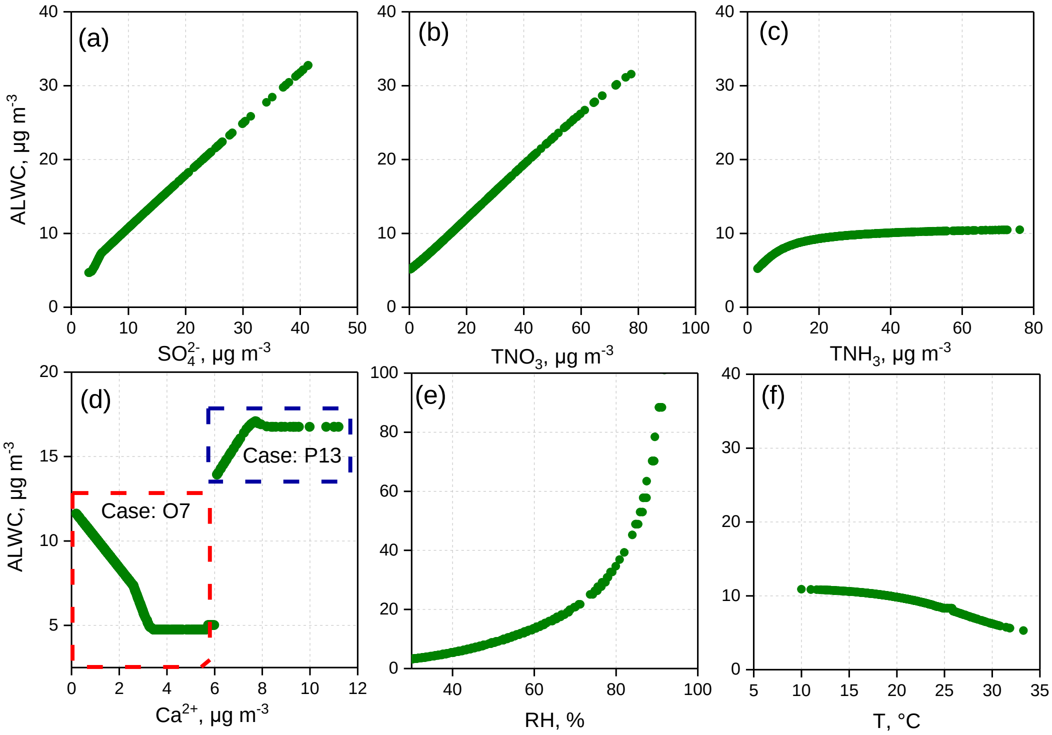

Figure S10. Sensitivity tests of ALWC to SO_4^{2-}, TNO_3, TNH_3, Ca^{2+}, and meteorological parameters (RH and T) in spring. For the sensitivity of ALWC to Ca^{2+}, in ISORROPIA-II, subroutine O7 was automatically called when the Ca^{2+} mass concentration was low and the subroutine P13 was automatically called when the Ca^{2+} mass concentration was high.

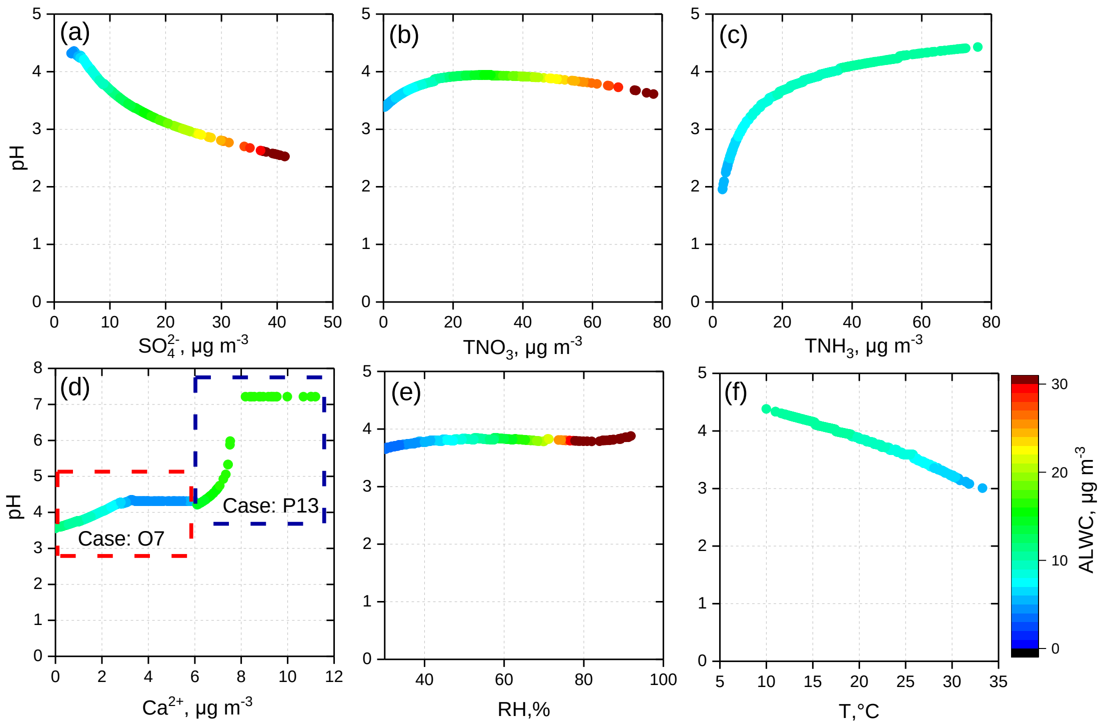

Figure S11. Sensitivity tests of $PM_{2.5}$ pH to SO_4^{2-}, TNO_3, TNH_3, Ca^{2+}, and meteorological parameters (RH and T) in spring. For the sensitivity of $PM_{2.5}$ pH to Ca^{2+}, in ISORROPIA-II, subroutine O7 was automatically called when the Ca^{2+} mass concentration was low while the subroutine P13 was automatically called when the Ca^{2+} mass concentration was high.

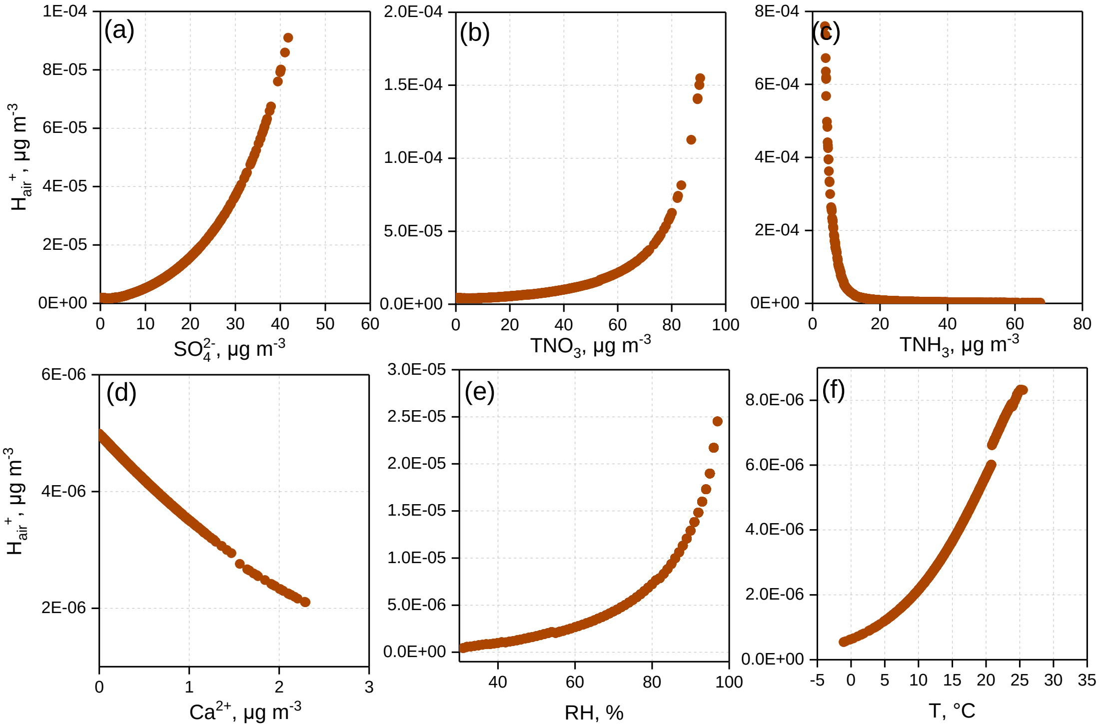

Figure S12. Sensitivity tests of H_{air}^{+} to SO_4^{2-}, TNO_3, TNH_3, Ca^{2+}, and meteorological parameters (RH and T) in autumn.

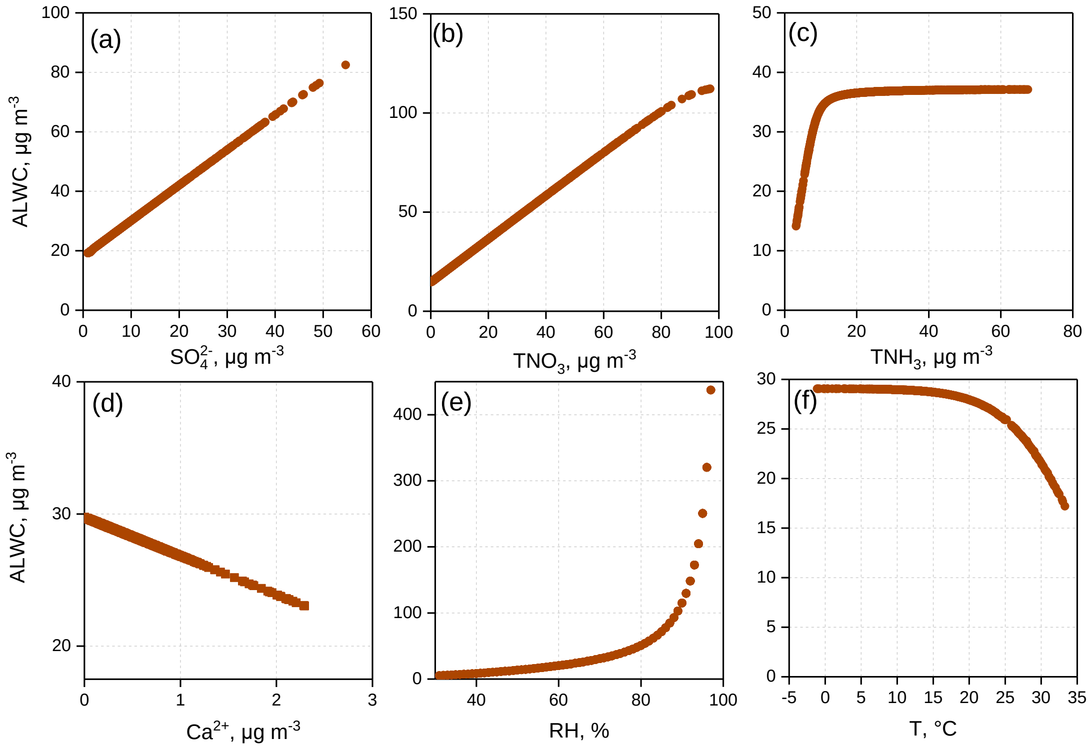

Figure S13. Sensitivity tests of ALWC to SO_4^{2-}, TNO_3, TNH_3, Ca^{2+}, and meteorological parameters (RH and T) in autumn.

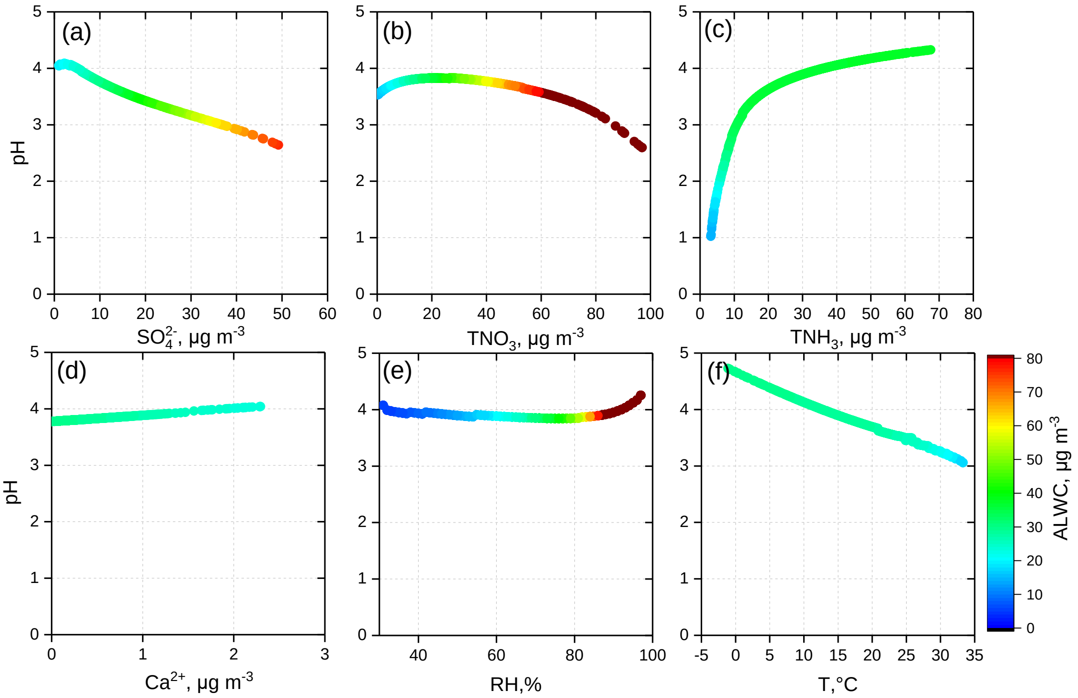

Figure S14. Sensitivity tests of $PM_{2.5}$ pH to SO_4^{2-}, TNO_3, TNH_3, Ca^{2+}, and meteorological parameters (RH and T) in autumn.

4. Rich-ammonia in the North China Plain

The ratio of [TA]/2[TS] provides a qualitative description for the ammonia abundance, where [TA] and [TS] are the total (gas + aqueous + solid) molar concentrations of ammonia and sulfate. The rich-ammonia is defined as [TA] > 2[TS], while if the [TA] ≤ 2[TS], then it is defined as poor-ammonia (Seinfeld and Pandis, 2016). In this work, the ratio of [TA]/2[TS] was much higher than 1 and belonged to rich-ammonia conditions (Figure S15). Figure S15 shows that the nitrate mass concentration did not always increase with elevated ammonia, demonstrating that the nitrate formation is limited by nitric acid in the North China Plain rather than ammonia.

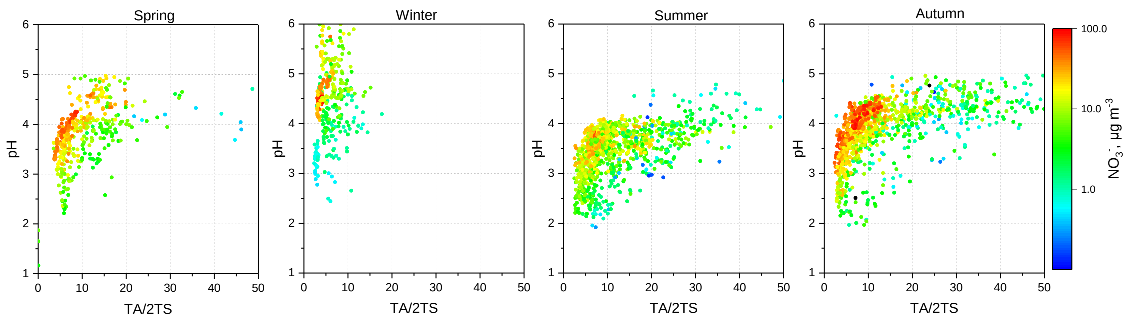

Figure S15. Predicted $PM_{2.5}$ pH colored by NO_3^- mass concentration versus measured TA/2TS ratio (mole mole^{-1}) over four seasons (data at RH≤30% were excluded).

References

Seinfeld, J. H., Pandis, S. N.: Atmospheric Chemistry and Physics: From Air Pollution to Climate Change, John Wiley & Sons, Inc., Hoboken, New Jersey, USA, 2016.

5. Sensitivity tests of gas-particle partitioning to TNO_3, TNH_3, RH, and T in spring and autumn.

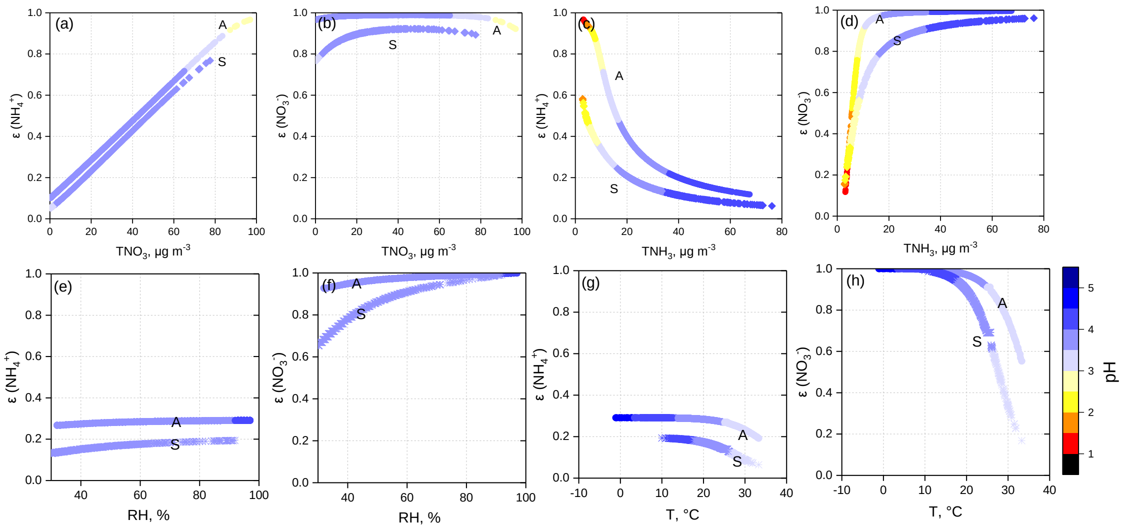

Figure S16. Sensitivity tests of ε(NH_4^+), ε(NO_3^-), and ε(Cl^-) to TNO_3, TNH_3, RH and T coloured by $PM_{2.5}$ pH in spring (S) and autumn (A).

6. Size-resolved aerosol pH in the daytime and nighttime.

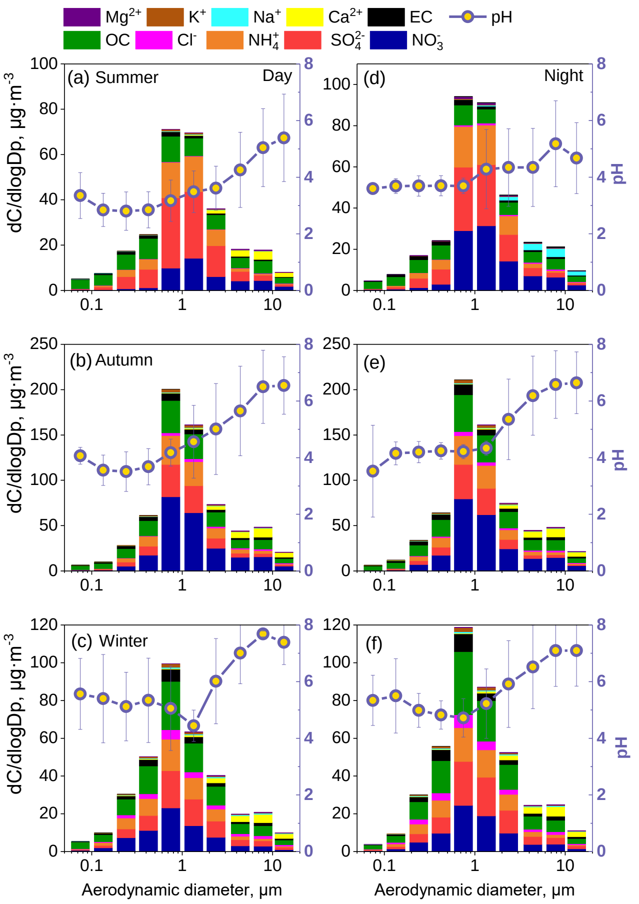

Figure S17. Size-resolved aerosol pH and all analyzed chemical components in daytime (a, c, e) and (b, d, f) nighttime in summer, autumn, and winter.

6. Sensitivity tests of size-resolved aerosol pH to Ca^{2+}.

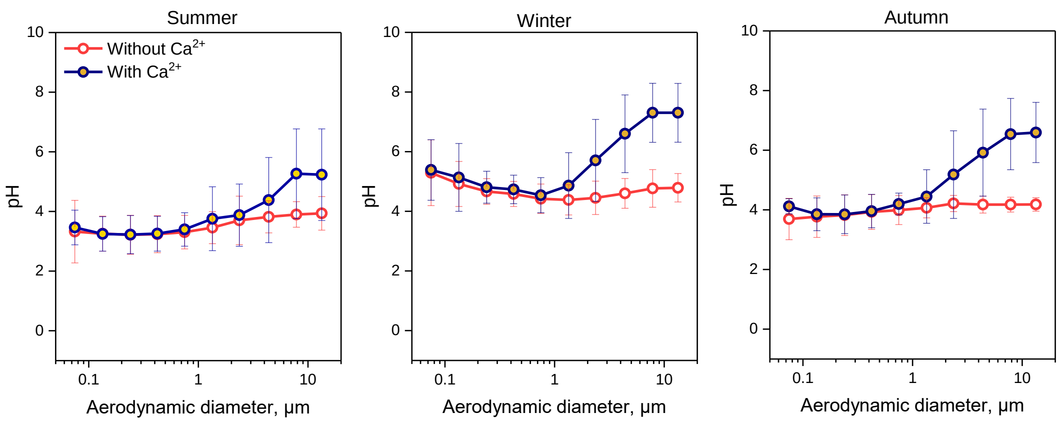

Figure S18. Size-resolved aerosol pH with and without Ca^{2+} in summer, winter, and autumn.